Analysis of flow characteristics and development recommendations for Karst Geothermal reservoirs based on tracing experiment: A case study of Fanxian geothermal field

Kefu Li[1,2]*, Chuanqing Zhu[1,2], Yongwang Zhang[1,2]
State Key Laboratory of Deep Geothermal Resources, Beijing, China[1], College of Geosciences, China University of Petroleum, Beijing, China[2]
*Corresponding author: likefu553@163.com

INTRODUCTION

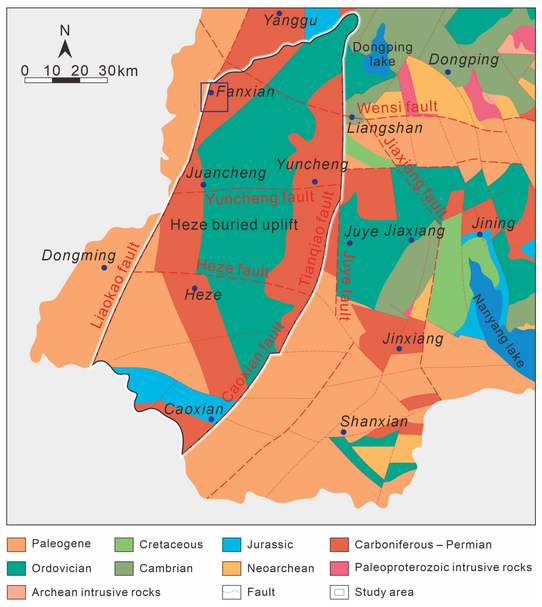


Figure 1. Tectonic setting of the Fanxian geothermal field

The study area is located at the junction of the Dongming Depression and the Luxi Uplift within the Heze Sub-uplift, controlled by major faults such as the Lanliao and Wensi faults (Fig. 1). The structure is complex with well-developed fault systems. The geothermal field is characterized by a sub-uplift type carbonate reservoir within a sedimentary basin, consisting mainly of porous and fracture cavity composite media. The reservoir roof is buried at depths of 400–1600 m, with a geothermal gradient of 2.6–3.4 °C/100 m and water temperatures of 45–70 °C. The maximum single-well discharge reaches 183 m³/h. Hydrochemical types are mainly Cl–Na and SO_4·Cl–Na·Ca. The geothermal water is primarily recharged by atmospheric precipitation from the Liangshan–Jiaxiang mountainous area, flowing generally from east to west and northeast to southwest (Kang et al., 2024).

METHODS

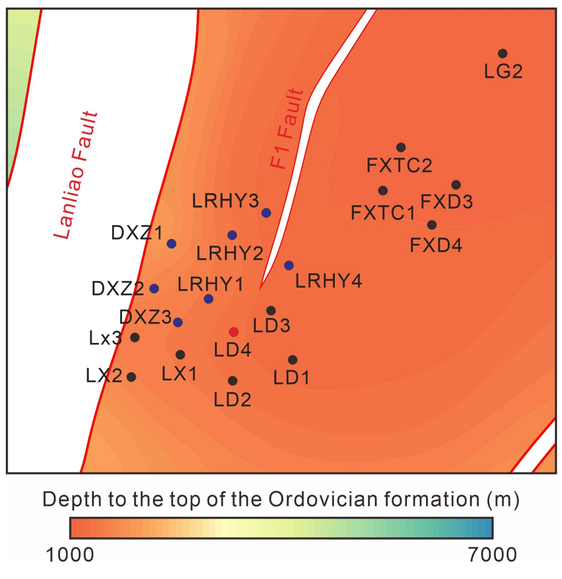


Figure 2. Well distribution in the Fanxian geothermal field

Sodium fluorescein was used as the tracer, and the test began on December 17, 2024. A total of 50 kg of tracer was dissolved in 3 t of reinjection water and rapidly injected into the reinjection well LD4 using a constant-flow pump. A dynamic sampling strategy was applied: samples were collected every 12 h initially, every 5 h after tracer detection, and reverted to 12 h when concentrations were low or below detection. Seven monitoring wells (LRHY1–4 and DXZ1–3) were observed (Fig. 2), with production rates of 110–130 m³/h and discharge temperatures of 50–70 °C. The injection well lies 500–1500 m from the monitoring wells. During the test, 1,146 water samples were collected and analyzed on-site using a handheld fluorometer (FluoroQuik), which provides high sensitivity, rapid response, and reliable detection for real-time monitoring of tracer concentrations.

RESULTS

Characteristics of the Concentration-Time Curve

The tracer concentration–time curves of seven monitoring wells all showed a three-peak pattern (Fig. 3). Tracer was detected in all wells at the first measurement, indicating well-developed, highly permeable karst channels in the Fan County geothermal field. Peaks appeared at 45–76 h, 143–164 h, and 187–220 h, with concentrations of 0.66–1.60, 0.81–1.40, and 0.28–0.73 μg/L, the second peak being the highest, suggesting better storage and permeability in those channels. The multi-peak response reflects three heterogeneous karst channel systems between monitoring and reinjection wells, affecting tracer migration paths and concentration distribution.

Tracer Seepage Velocity

In tracer experiments, apparent velocity is defined as the tracer migration rate at peak concentration (Goldscheider et al., 2008). For the seven monitoring wells, velocities for the three peaks ranged 8.55–29.59, 4.55–11.69, and 2.95–7.59 m/h (Fig. 3). Well DXZ1, northwest of the injection well, had the highest velocities (29.59, 11.69, 7.59 m/h) with peak concentrations of 0.89, 1.40, and 0.72 μg/L, while LRHY1, north of the injection well, had the lowest (8.55, 4.55, 2.95 m/h) with 0.77, 1.00, and 0.28 μg/L. The increasing concentration differences across peaks and the marked second-to-third peak difference in LRHY1 reflect strong directional variability and heterogeneity in the Fanxian geothermal groundwater system.

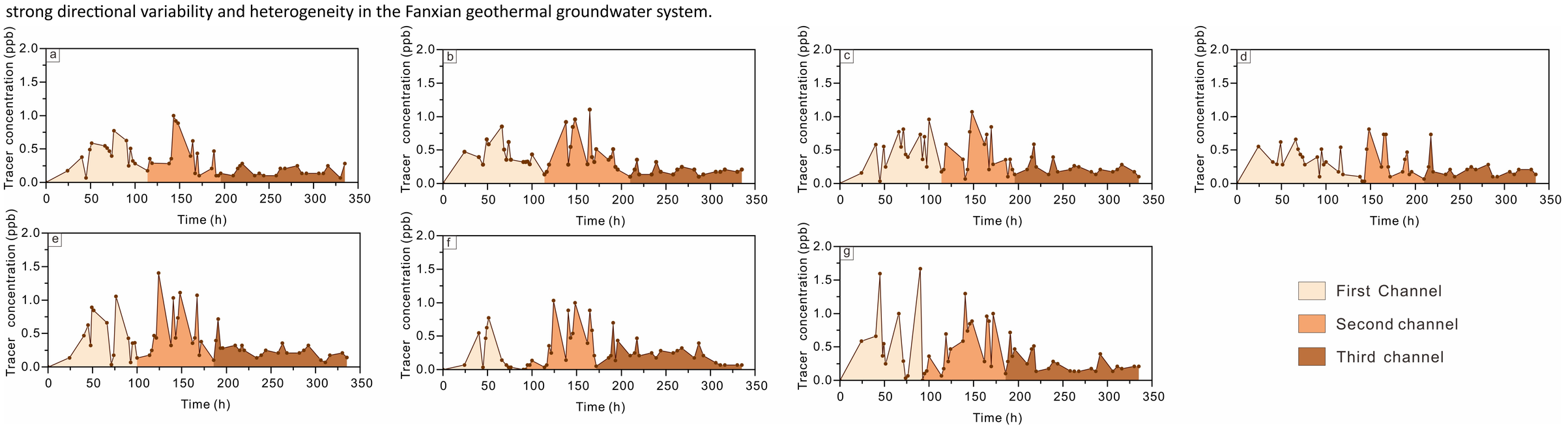


Figure 3. Fluorescein concentration curves from the seven monitoring wells.

DISCUSSION

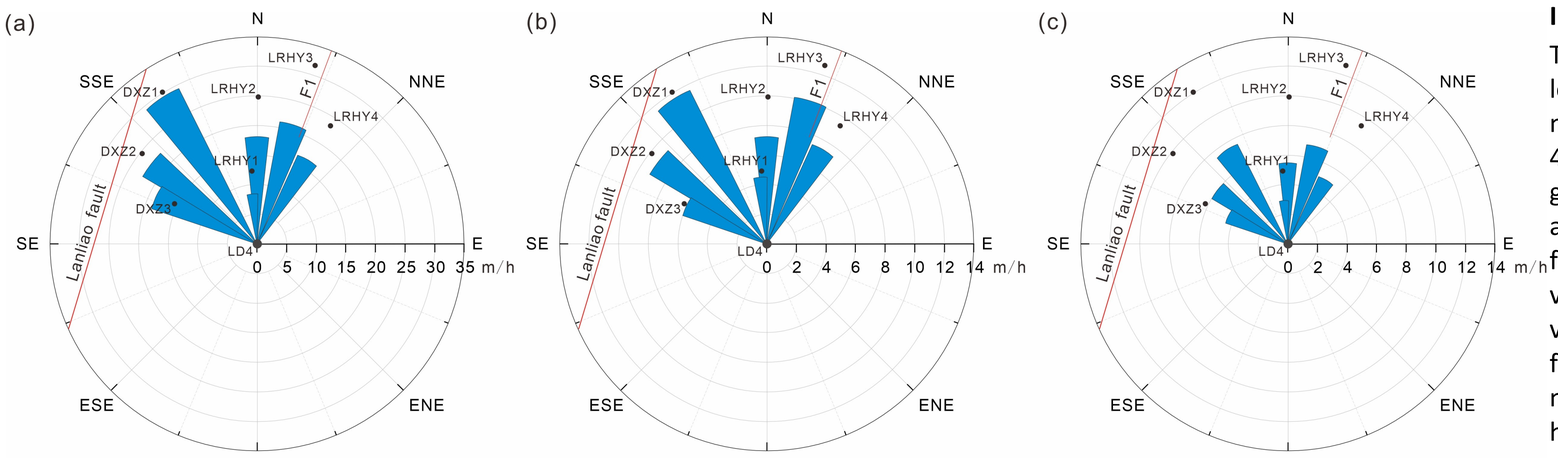


Figure 4. Radar plot of apparent velocities for the Ordovician karst geothermal reservoir based on monitoring well data. a. First channel; b. Second channel; c. Third channel.

Influence of fault on the karst geothermal reservoir flow system

The flow velocity radar chart (Fig. 4) shows a maximum apparent flow velocity of 29.59 m/h, with preferential flow in all three conduits directed northwest. The area is mainly controlled by the deep Lanliao fault (600–4200 m displacement) and secondary fault F1 (60–100 m). High-velocity regions align with the Lanliao fault, indicating its key role in enhancing storage and transmission in the Ordovician karst reservoir, while F1 mainly forms local fracture networks. Fault effects are reflected in monitoring well velocities, LRHY2, farther from the injection well but near F1, shows higher velocities than LRHY1, suggesting that structural stress near F1 promotes fracture development and improves flow connectivity. Similarly, in the northwest-oriented DXZ well cluster, DXZ1, closer to the Lanliao fault, exhibits higher velocities than DXZ3, confirming that proximity to major faults enhances fracture development and flow capacity. These patterns demonstrate that fault structures strongly control karst conduit development and the regional geothermal flow system, with deeper faults forming highly connected channels and secondary faults contributing local enhancements, collectively governing apparent flow velocities and overall reservoir performance (Bili et al., 2003; Olierook et al., 2014; Haines et al., 2016).

CONCLUSION

(1)The Fanxian geothermal field's karst reservoir exhibits a heterogeneous flow system, with three distinct karst conduit groups existing between production and injection wells.

(2)The differences in velocities and peak concentrations among the three conduits indicate that the second conduit has the best storage and permeability, with higher tracer retention and peak concentration.

(3) Regional fault structures exert significant control over the reservoir flow system, enhancing fracture development and karst conduit connectivity in surrounding areas.

Acknowledgements

This study was financially supported by the National Key Research and Development Program of China (2021YFA0716003).

REFERENCES

Goldscheider, N., Meiman, J., Pronk, M., Smart, C.,: Tracer tests in karst hydrogeology and speleology. International Journal of Speleology, 37, (2008), 27–40.

Kang, F., Ma, Z., Shi, M., Liu, X., Huang, H.,: Renewable capacity of karst geothermal water and production-reinjection balanced resources evaluation: A case study of Heze buried uplift geothermal fields. Earth Science (in Chinese) 48, (2023), 1118–1137.

Billi, A., Salvini, F., Storti, F.,: The damage zone-fault core transition in carbonate rocks: implications for fault growth, structure and permeability. Journal of Structural Geology, 25, (2003), 1779–1794.

Olierook, H.K.H., Timms, N.E., Hamilton, P.J.,: Mechanisms for permeability modification in the damage zone of a normal fault, northern Perth Basin, Western Australia. Marine and Petroleum Geology, 50, (2014), 130–147.

Haines, T.J., Michie, E.A.H., Neilson, J.E., Healy, D.,: Permeability evolution across carbonate hosted normal fault zones. Marine and Petroleum Geology, 72, (2016), 62–82.